

Kinematics of diving Atlantic puffins (*Fratercula arctica* L.): evidence for an active upstroke

L. Christoffer Johansson* and Björn S. Wetterholm Aldrin

Department of Zoology, Göteborg University, Box 463, SE-405 30 Göteborg, Sweden

*e-mail: christoffer.johansson@zool.gu.se

Accepted 26 November 2001

Summary

To examine the propulsion mechanism of diving Atlantic puffins (*Fratercula arctica*), their three-dimensional kinematics was investigated by digital analysis of sequential video images of dorsal and lateral views. During the dives of this wing-propelled bird, the wings are partly folded, with the handwings directed backwards. The wings go through an oscillating motion in which the joint between the radius-ulna and the hand bones leads the motion, with the wing tip following. There is a large rotary motion of the wings during the stroke, with the wings being pronated at the beginning of the downstroke and supinated at the end of the downstroke/beginning of the upstroke. Calculated instantaneous velocities and accelerations of the bodies of the birds show that, during the downstroke, the birds accelerate upwards and forwards. During the upstroke, the birds accelerate downwards and, in some sequences analysed, also

forwards, but in most cases the birds decelerate. In all the upstrokes analysed, the forward/backward acceleration shows the same pattern, with a reduced deceleration or even a forward acceleration during 'mid' upstroke indicating the production of a forward force, thrust. Our results show that the Atlantic puffin can use an active upstroke during diving, in contradiction to previous data. Furthermore, we suggest that the partly folded wings of diving puffins might act as efficient aft-swept wingtips, reducing the induced drag and increasing the lift-to-drag ratio.

A movie is available on-line.

Key words: puffin, *Fratercula arctica*, Alcidae, alcid, swimming, diving, locomotion, kinematics.

Introduction

Underwater wing propulsion among birds is quite common and has evolved on several separate occasions. Among the wing-propelled birds, the penguins are the most specialized (Storer, 1960a; Clark and Bemis, 1979; Bannasch, 1995), with an almost entirely aquatic lifestyle and the loss of aerial flight ability. Among the less-extreme wing-propelled divers, we find a variety of birds including diving petrels (Pelecanoididae) (Ryan and Nel, 1999), dippers (Cinclidae) (Goodge, 1959), some ducks (Anatidae) (Humphrey, 1958; Hawkins et al., 2000) and alcids (Alcidae) (Stettenheim, 1959; Spring, 1971). All these birds retain the ability to fly in air, although diving petrels and alcids have been considered to be intermediate stages towards a totally aquatic life style (Storer, 1960a).

The use of wings for both aerial flight and underwater propulsion puts conflicting selection pressures on wing morphology. In air, low flight power requirements are achieved by having long, narrow wings with low wing loading and a high aspect ratio (Norberg, 1996). The density of sea water is 850 times that of air, which affects force production, making lift and drag four times larger in water than in air at the same Reynolds number (Vogel, 1994). The difference in density also affects the added mass, which increases the inertia of the wings

(Ellington, 1984; Vogel, 1994) and the biomechanical demands on the wing bones, pectoral muscles (Lovvorn and Jones, 1994) and flight feathers. Together, these effects make short, high-aspect-ratio wings more favourable in water to allow high swimming speeds at low cost.

The alcids have met these conflicting selection pressures by using partially folded wings while diving (Stettenheim, 1959; Spring, 1971). Furthermore, alcids have relatively small wings which, it has been suggested, are an adaptation to underwater flight (Storer, 1960b). Lovvorn and Jones (1994) argued that the small wings of diving birds, in general, might not represent an adaptation to diving or high-speed flight, as was suggested by Rayner (1988). Instead, they argued that relaxation of selection for manoeuvrability, because of the damped impact of landing on water, was a more likely reason for their small wings. A more probable selection pressure for small wings in diving birds may be the reduction in buoyancy; this is supported by the relatively smaller wings of diving ducks compared with those of other ducks (Rayner, 1988). This mechanism for buoyancy reduction might be particularly important since reduction in wing size does not increase the total inertia of the birds, in

contrast to some other suggested methods of buoyancy reduction (Lovvorn and Jones, 1994).

Underwater wing propulsion has been thoroughly studied in penguins (Clark and Bemis, 1979; Hui, 1988; Bannasch, 1995). These birds use an active, thrust-producing upstroke as well as an active downstroke in forward propulsion (Clark and Bemis, 1979; Hui, 1988). Penguins have relatively large supracoracoid muscles (Dabelow, 1925; Kovacs and Meyers, 2000), which allows them to produce a large force during the upstroke (Hui, 1988). The relatively large ratio of supracoracoid muscle mass to flight muscle mass in alcids compared with other flying birds (Kovacs and Meyers, 2000) has led to the suggestion that the alcids might, like penguins, use an active upstroke while diving (Stettenheim, 1959; Lovvorn et al., 1999; Kovacs and Meyers, 2000). The suggested mechanism has been compared with that of a paddle (drag-based), which would keep the birds from floating to the surface (Stettenheim, 1959), but the upstroke has also been modelled as active and thrust-generating (Lovvorn et al., 1999). Until now, the available hydrodynamic data have indicated a non-active upstroke in diving alcids (Rayner, 1995). Our aim here is to explore whether the kinematics of diving Atlantic puffins provides support for an active upstroke in alcids and whether the force produced could be drag-based.

Materials and methods

Animals

The study was conducted on the Vestman Islands (Iceland), using six Atlantic puffins (*Fratercula arctica* L.) captured on the day of the study. The study was approved by the Icelandic Ministry for the Environment (UMH00030179/13-4-1 HG/—).

Morphometrics

The wing span (tip to tip measured on outstretched wings), wing length (from body to wing tip), wing area (including the body segment between the wings), single wing area (area of one wing without the body segment), chord (wing area/wing span), aspect ratio $[(\text{wing span})^2/\text{wing area}]$ and aspect ratio of a single wing $[(\text{wing length})^2/\text{single wing area}]$ were measured from photographs using Scion Image for Windows 2000. The tarsus was measured as the distance between the hypotarsus and the condyle of the third toe on the tarsus. The mass of each bird was measured after completion of the study.

Experimental arrangement

The study was conducted in a tank 5 m × 1 m × 1 m (length × width × depth), filled with sea water. The tank was built using waterproof plywood sealed with silicone and sealant. It was covered by a net to prevent the bird from escaping and to restrict the bird from surfacing other than at the ends of the tank. The measuring section consisted of a 1 m long × 0.6 m wide window in the middle of one of the long sides of the tank and a 1 m long section on the top marked with a grid of 0.02 m × 0.02 m. A window at one of the ends enabled filming

of the frontal and caudal views. The birds were stimulated to dive from one end of the tank to the other by the approach of an experimenter. Filming was conducted using a Hi-8 Sony video camera (CCD-TR705E) and a Hi-8 Canon video camera (UC-X50HiE). The birds were filmed from the lateral view, and most birds were also filmed from either the dorsal or frontal/caudal view.

Image analysis

The video sequences were captured, using a Pinnacle Systems (miroVideo DC-30) framegrabber. The images were separated into frames (resulting in 50 frames s⁻¹) and contrast-enhanced using Adobe Photoshop 5.5. The stacks of frames were then analysed using Scion Image. Sequences from all six birds were used in the analysis. Only sequences in which the birds swam using synchronized wing strokes without apparent turns were used, and all the sequences analysed contained at least one complete wing stroke. Both dorsal and lateral views were used for the three-dimensional kinematic description. The views were synchronised manually by examining the velocity and acceleration curves of the dorsal and lateral views. This procedure may result in a small timing error, which would not affect our results other than those presented in Fig. 4 as this is the only figure in which information from both views is combined. For all other analyses, only information from the lateral view was used.

From the lateral view, six points were measured in each frame: the tip of the tail (Tail), the eye (Eye), the border between the white belly and the black breast band (Breast), the tip of the beak (Beak) and two points on the wing closest to the lateral camera. These latter marks were the tip of the wing (Tip) and the joint between the radius-ulna and the hand bones (Wrist). From the dorsal view, six points were measured in each frame: the tip of the tail (Tail), the base of the beak (BeakBase), two points on the wing furthest from the lateral camera and two points on the wing closest to the camera. These latter marks were the tip of the distal wing (DistTip), the tip of the proximal wing (Tip), the joint between the radius-ulna and the hand bones of the distal wing (DistWrist) and this joint on the proximal wing (Wrist). The eye and the tail were taken as a fixed body points for the lateral and dorsal view, respectively.

Data analysis

The mean swimming speed (V) of the bird was calculated as the average distance travelled during an entire wing stroke for an analysed sequence divided by the duration of the stroke. This speed was used to calculate the Reynolds number Re $[=lV/\nu]$, where l is length, V is speed and ν is the kinematic viscosity of sea water] using the total body length of the bird (from the tip of the beak to the tail tip). A least-squares regression coefficient for 24 sequences (each sequence by six birds was taken as an independent dive for regression analysis) was calculated (using SigmaPlot) for mean swimming velocity (V) versus stroke frequency (f) to determine whether speed increases with stroke frequency. A least-squares regression coefficient was also calculated for mean velocity versus stride length (l_s), which was

Table 1. Morphological and kinematic variables (see text for definitions) of six Atlantic puffins (*Fratercula arctica*)

Mass (kg)	0.446±0.0125 (6)
Tarsus length (m)	0.0277±0.00026 (6)
Wing span (m)	0.589±0.0042 (6)
Wing area (m ²)	0.03714±0.00054 (6)
Mean chord (m)	0.0631±0.00065 (6)
Aspect ratio	9.3±0.11 (6)
Wing length (m)	0.242±0.0021 (12)
Single wing area (m ²)	0.01519±0.00017 (12)
Aspect ratio of a single wing	3.9±0.038 (12)
Ratio of downstroke duration to total Stroke duration	0.39±0.014 (24)

Values are means ± S.E.M. (N).

calculated as the distance travelled during one stroke cycle. The dive angle was measured as the direction of movement of the body with respect to the background [the arctan of the vertical (y) distance travelled divided by the horizontal (x) distance travelled during a complete wing stroke]. A least-squares regression was calculated for the downstroke fraction of the stroke duration *versus* dive angle to test whether the relative duration of the downstroke varied with dive angle. The stroke amplitudes of the Tip (A_T) and Wrist (A_W) in the y direction were measured as the maximum deviation with respect to the fixed body point (Eye). The relationships between A_T or A_W and mean velocity were tested using a least-squares regression. The mean acceleration (a_V) was calculated as the change in mean velocity during the analysed sequence, and least-squares regressions of mean acceleration *versus* stroke frequency and A_T or A_W were calculated. All the slopes were tested for significant ($P < 0.05$) deviation from zero.

The mean instantaneous swimming speed and acceleration in the x and y directions of three body points (Beak, Breast and Eye) were calculated by using five- and seven-point smoothing equations (Lanczos, 1956) for speed and acceleration, respectively.

Values are presented as means ± S.E.M.

Results

Morphological variables are presented in Table 1. Despite random sampling, all six birds were female with a mean mass (M) of 0.446±0.0125 kg and a mean tarsus length of 0.0277±0.00026 m. Video images of one of the diving puffins are shown in Fig. 1. The lateral (x,y) and dorsal (x,z) views of the movements of seven digitised points (Tail, Beak, BeakBase, Wrist, Tip, DistWrist and DistTip) with respect to the water, are plotted in Fig. 2. The paths of the measured points, with respect to the fixed body points of the dorsal (Tail as fixed body point) and lateral (Eye as fixed body point) views are plotted in Fig. 3. Figs 2 and 3 are based on the sequence illustrated in Fig. 1 and show approximately 1.5 stroke cycle. A three-dimensional representation of the kinematics is shown in Fig. 4 (see <http://www.biologists.com/JEB/movies/jeb3799.html>).

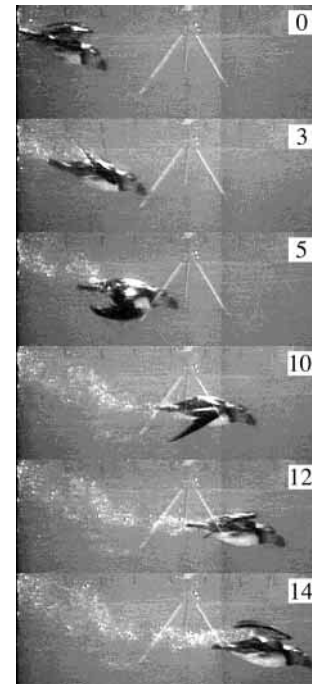


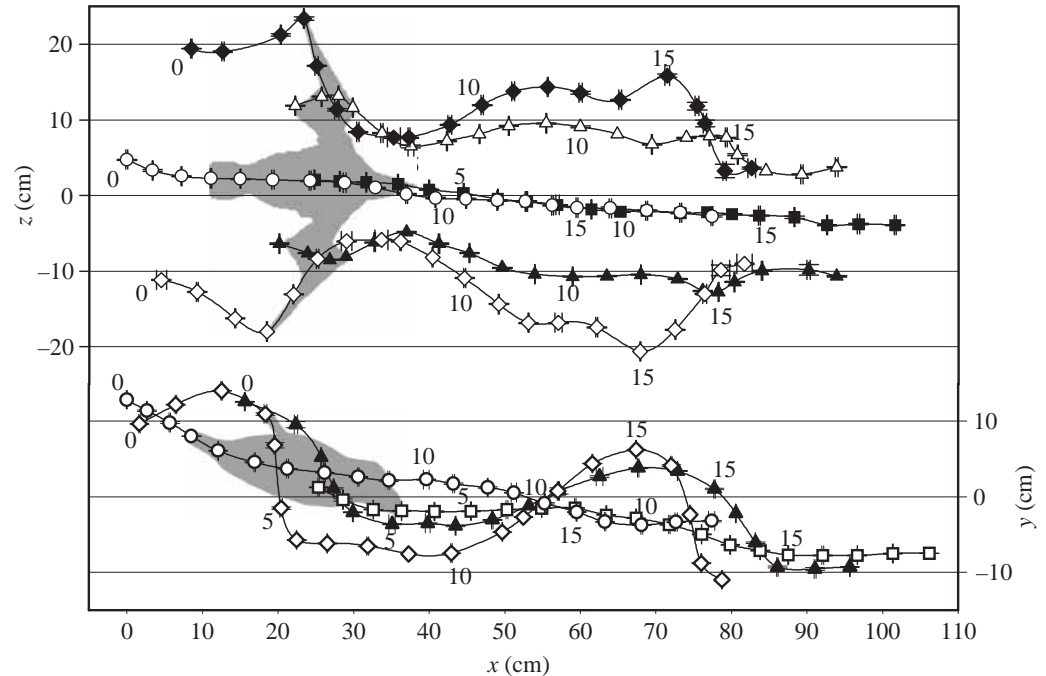
Fig. 1. Lateral-view video images from the sequence of a diving puffin used to generate Figs 2–4 and 5A,B. Frame numbers correspond to the numbers used in Figs 2 and 3.

Kinematics

The kinematics of the diving puffin was characterized by an oscillating movement of the wings in which the wrist (Wrist) leads and the wing tip (Tip) follows (Figs 2–4). The amplitude in the y direction of Tip was larger than the amplitude of Wrist (Fig. 3) in all the sequences analysed. This was also true for the z amplitude (Fig. 3) in three dorsal sequences analysed.

At the start of the downstroke, the wing undergoes a large pronating motion, as a consequence of the wrist (Wrist) initiating the downward motion while the wing tip (Tip) is still moving upwards. As a result, the rotation point of the handwing lies between the wrist and the wing tip. The rotation point is ventral to the maximum turning point of both the wrist (Wrist) and the wing tip (Tip), which gives a lower amplitude of the rotation point. During the downstroke, the wing is moved downwards, medially and slightly backwards with respect to the body (Fig. 3) and the wing is moved downwards and forwards with respect to the water (Fig. 2). At the end of the downstroke (start of the upstroke), the wing goes through a supinating motion as the wrist (Wrist) starts moving laterally and dorsally while the wing tip (Tip) is still moving medially (Figs 3, 4). The bottom turning point is similar to the top turning point, the main difference being that the plane of the wing is directed ventrally instead of slightly dorsolaterally (Fig. 4). During the upstroke, the wing is moved laterally and dorsally and slightly forward with respect to the body (Fig. 3). At no point during the entire stroke does the wing move backwards with respect to the water (Fig. 2). During the upstroke, the wing length increases as it is unfolded (Fig. 4);

Fig. 2. Dorsal (x,z plane) and lateral (x,y plane) views of a sequence of a diving puffin relative to still water. Symbols mark the positions of digitised points (see text for definitions): ○, Tail; ■, BeakBase; □, Beak; ▲, Wrist; ◇, Tip; △, DistWrist; ◆, DistTip. Numbers in the graph correspond to frame numbers (see Fig. 1), each separated by 0.02 s. Values are means of three separate measurements, and error bars (S.E.M.) illustrate measurement error.



this process is reversed during the downstroke, and the wing length is reduced (Fig. 4).

Speed and acceleration

In six of the 24 sequences analysed, the instantaneous swimming speed and acceleration patterns show that the upstroke generates a positive acceleration in the x direction, indicating that a propulsive force (thrust) is produced (Fig. 5C). In two of these sequences, the acceleration reached values that were significantly higher than zero. Most sequences showed that the deceleration of the bird was reduced during mid upstroke (only one sequence showed a significantly negative acceleration during the mid upstroke), also suggesting that a forward-directed force was being generated (Fig. 5A). A similar pattern was observed irrespective of whether the birds were accelerating, decelerating or swimming at constant speed.

The speed and acceleration in the y direction show that the body of the bird oscillates up and down with respect to the mean dive path, moving upwards during the downstroke and downwards during the upstroke (Fig. 5B,D). The upward motion of the body lasts longer than the duration of the downstroke (Fig. 5B,D), as expected because of the upwardly directed buoyancy of the body.

Kinematic parameters

Swimming speed varied between 1.02 and 2.14 m s⁻¹ and stroke frequency between 2.17 and 4 Hz. The Reynolds number at the body (based on total body length) varied between 2.8×10^5 and 6.0×10^5 . The mean swimming speed (V) increased with increasing stroke frequency (f) ($V = 0.61 + 0.31f$; $r^2 = 0.30$, $P < 0.01$, $N = 24$) (Fig. 6A) and increasing stride length (l_s) ($V = 0.69 + 1.65l_s$; $r^2 = 0.24$, $P < 0.05$, $N = 24$) (Fig. 6B) but not with the amplitude of Wrist (A_w) (0.11 ± 0.002 m, $P = 0.27$,

$N = 24$) or Tip (A_T) (0.19 ± 0.0039 m, $P = 0.061$, $N = 24$). There was no effect of the relative duration of the downstroke (0.39 ± 0.014 , $N = 24$) on the dive angle ($P = 0.65$, $N = 24$). Mean acceleration (a_v) increased significantly with increasing stroke frequency ($a_v = -0.014 + 0.0064f$; $r^2 = 0.28$, $P < 0.01$, $N = 24$) (Fig. 6C), but was not affected by the amplitude of Wrist ($P = 0.36$, $N = 24$) or Tip ($P = 0.59$, $N = 24$). There was a significant negative effect of stroke frequency on stride length ($l_s = 0.74 - 0.074f$; $r^2 = 0.20$, $P < 0.05$, $N = 24$).

Discussion

Our results clearly show that the Atlantic puffin can use an active upstroke to gain thrust while diving, in contradiction to previous suggestions that alcids have an inactive upstroke (Rayner, 1995). Our findings might help to explain the relatively larger supracoracoid muscles found in alcids compared with other birds (Kovacs and Meyers, 2000). Large supracoracoid muscles indicate a more force-demanding upstroke, which would be the consequence of an active upstroke. Furthermore, we consider an active upstroke to be the only logical solution to the problem of positive buoyancy in these birds.

From viewing a sequence of a diving pigeon guillemot (*Cephus columba*), Rayner (1995) argued that alcids do not use an active upstroke because bubbles released from the feathers in the wings indicated the presence of vortex rings only during the downstroke. Rayner (1995) also argued that the force produced during the downstroke was directed primarily forwards, because the observed vortex rings were only slightly tilted relative to the vertical plane. A problem with this conclusion is that, because of the positive buoyancy of alcids (Lovvorn and Jones, 1991), a vertical vortex ring during the

downstroke, indicating a forward-directed force, would not allow the birds to remain submerged. A possible reason for Rayner's result is that it may be difficult for the air in the plumage to escape during the upstroke because the wing feathers are then oriented downwards, trapping the air in the plumage and thus failing to illuminate potential vortex rings. We were unable to observe bubble ring formation during the upstroke because few bubbles were released from the wings during this phase. An additional problem with observing bubbles released from the feathers is that bubbles released at the beginning of the upstroke will move upwards because of their own buoyancy, thus resulting in a ring of bubbles in a plane different from that expected.

Stettenheim (1959) suggested that the common murre (*Uria aalge*) uses the upstroke in a drag-based manner (like a paddle) to keep it from floating to the surface while swimming horizontally. From the images presented by Stettenheim (1959), it is possible to compare the wing motion of the murre with that of the puffin. We found that the motions with respect to the body are similar in the two species, suggesting that an active upstroke is also present in the common murre. Considering the approximate direction of the resultant velocity meeting the wings of the puffins, it is difficult to argue that the forward-directed thrust recorded during the upstroke could be generated by drag. During mid upstroke, the wings are moving upwards and forwards with respect to the water, directing drag backwards and downwards. Any lift force generated would be directed upwards and backwards or downwards and forwards. The generation of a lift force directed downwards and forwards during the upstroke would explain the observed thrust and downward acceleration. The formation of such a lift force could be the result of a 'horizontal' vortex ladder similar to that suggested by Bannasch (1995) for penguins. The main differences, compared with the penguin, would be that the vortex formed during the upstroke would be larger than the vortex formed during the downstroke (because the upstroke represents a larger proportion of the stroke duration) and that the vortex of the upstroke would be at a shallower angle with respect to the direction of the dive.

During diving, the wings of alcids are partly folded, with the primary feathers in a multi-laminate structure, forming the backswept wing tip. The multi-laminate structure probably increases the bending resistance of the wing tip, helping the feathers to endure potentially increased biomechanical demands, compared with air, because of the decreased bending resistance of wetted feathers (B. S. Wetterholm Aldrin,

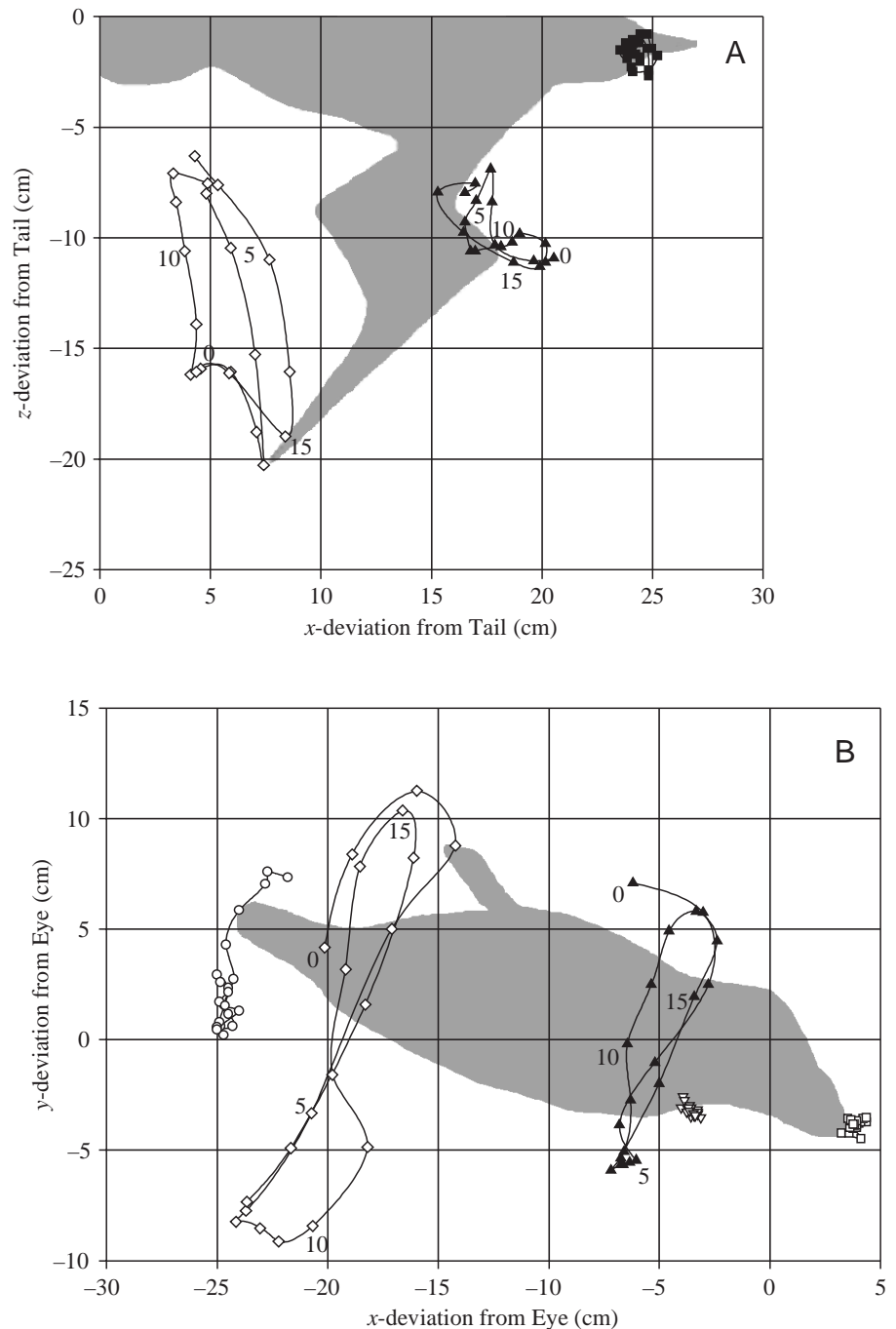


Fig. 3. (A) Dorsal view (x,z plane) and (B) lateral view (x,y plane) of the wing movement relative to the movement of the tail tip (Tail) and eye (Eye) respectively. Symbols mark the positions of digitised points (see text for definitions): \circ , Tail; \blacksquare , BeakBase; \square , Beak; ∇ , Breast; \blacktriangle , Wrist; \diamond , Tip. Numbers in the graph correspond to frame numbers (see Fig. 1), each separated by 0.02 s.

personal observations) and added mass considerations. The folded wing of diving alcids may result in the handwings functioning as aft-swept wing tips, which has been shown to reduce induced drag during flight (van Dam, 1986, 1987; Burkett, 1989) and increase the lift-to-drag ratio (van Dam et al., 1991b), resulting in a more forward-directed resultant force. Aft-swept wings also show superior properties under non-steady-state conditions (Liu and Bose, 1999), including a reduction of lift loss at angles of attack causing flow separation (van Dam et al., 1991a). Thus, the aft-swept wings of puffins might not simply represent an intermediate stage towards flightlessness, and penguin-like flippers but might be an adaptation generating more thrust and representing a more hydrodynamically stable system.

The mean forward swimming speed of the puffins increased with stroke frequency and stride length (distance travelled during a stroke) (Fig. 6A,B), as in penguins (Clark and Bemis,

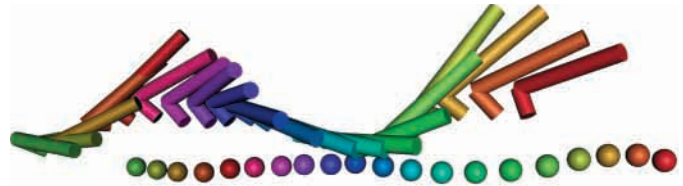


Fig. 4. Three-dimensional representation of the left wing of an Atlantic puffin (*Fratercula arctica*) during diving. The spheres represent the position of the tail tip (Tail) and the rods represent the line between the wrist (Wrist) and the wing tip (Tip) and between the wrist and the elbow. The motion goes from right to left (i.e. starting with the red colour and ending with the green colour). The printed version and the start image of the movie (see <http://www.biologists.com/JEB/movies/jeb3799.html>) shows a ventral/lateroventral view. The three-dimensional coordinates were produced according to the specifications in the Materials and methods section.

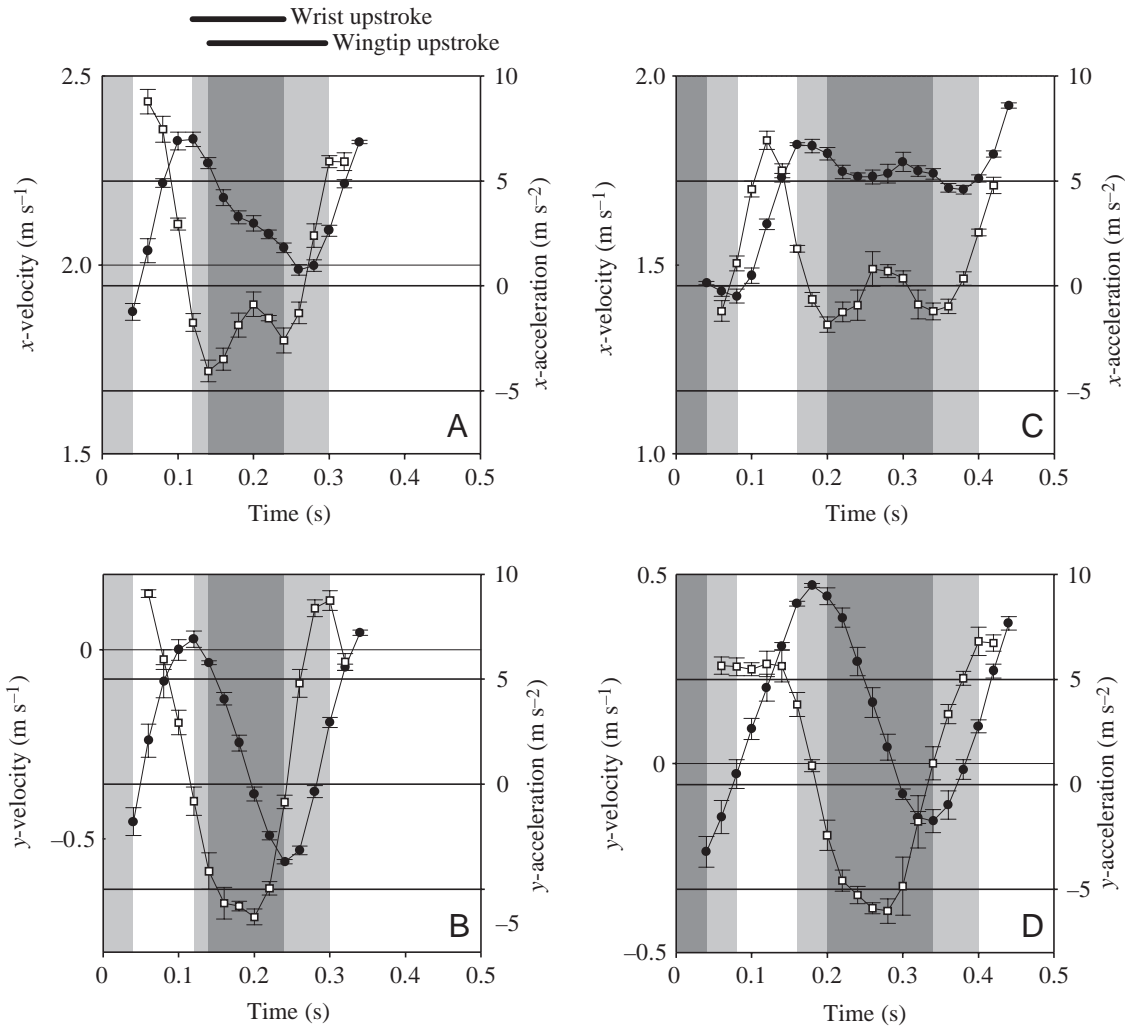


Fig. 5. Velocity (●) and acceleration (□) in the x (A) and y (B) directions of the puffin in the sequence used in Figs 2–5 and in the x (C) and y (D) directions of a bird in a sequence showing positive acceleration in the x direction during the upstroke. The upstroke of the wrist point (Wrist) is from the start of the light grey area to the end of the dark grey area. The upstroke of the wing tip (Tip) is from the start of the dark grey area to the end of the light grey area. The values are means of the velocity and acceleration of three digitised points on the body (Beak, Eye and Breast) and error bars are \pm S.E.M. (see text for definitions).

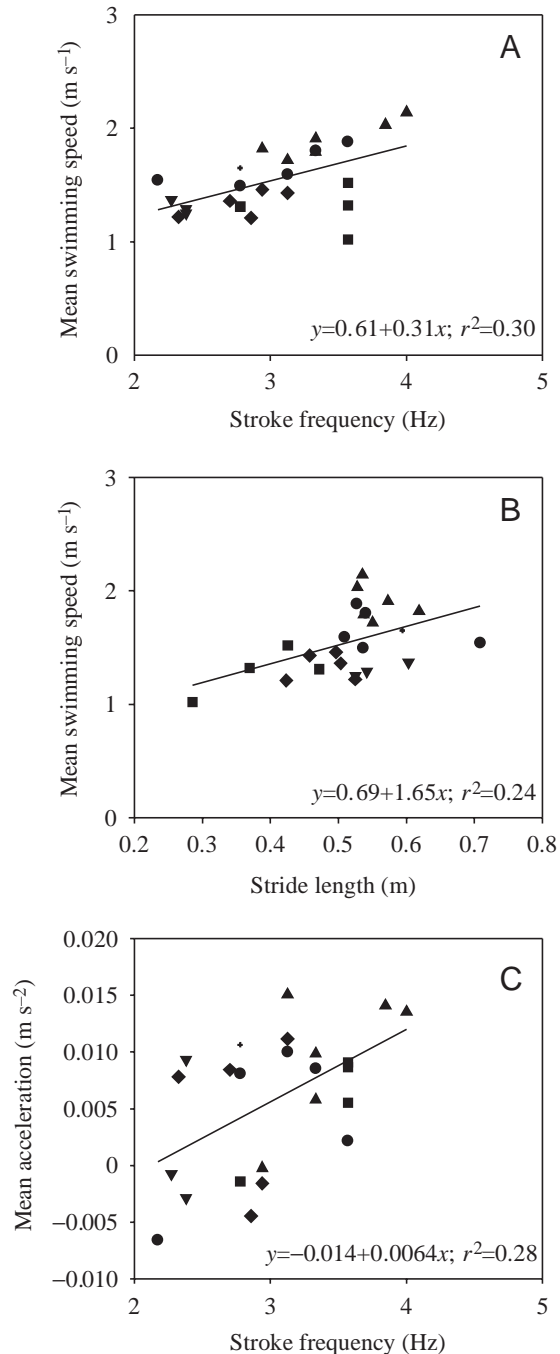


Fig. 6. Graphs showing the relationships between (A) stroke frequency and mean swimming speed, (B) stride length and mean swimming speed and (C) stroke frequency and mean acceleration. The different symbols represent six different individuals. The regression coefficients in A, B and C are significantly greater than zero.

1979). In puffins, the mean speed did not increase significantly with stroke amplitude of the wing tip or wrist, although there was a trend towards an increase with the amplitude of the wing tip (A_T , $P=0.061$). The relatively high stroke frequencies recorded here (mean 3.0 Hz), compared with those reported for thick-billed murres *Uria lomvia* (1.8 and 1.9 Hz) (Croll and

McLaren, 1993), could be a consequence of mass differences. On the basis of stroke frequency data from Clark and Bemis (1979) and the body mass measurements of Watanuki and Burger (1999), we found a significant negative power regression between stroke frequency (f) and body mass (M) ($f=4.1M^{-0.25}$; $r^2=0.76$, $P<0.05$, $N=7$) for penguins. Common murres are approximately 70% larger than puffins and, assuming the same regression coefficient for alcids as for penguins, this would account for approximately 30% of the difference in stroke frequency. However, our kinematic data suggests a different, non-steady-state mechanism in alcids possibly resulting in a different relationship between frequency and mass. Alternatively, the differences could result from our experimental procedures. Because the birds were stimulated to dive by us approaching them, the dives could be regarded as escape dives. During escape, it would be favourable to accelerate fast and swim at high speed, which can be achieved with a high stroke frequency.

Furthermore, our result provides support for the assumptions in the model of alcid diving of Lovvorn et al. (1999). Their model assumes an active upstroke, which is responsible for a significant proportion of the thrust produced. Although our results suggest an active upstroke, they also indicate that Lovvorn et al. (1999) may have overestimated the effect of the upstroke. However, our experiment was conducted at a shallow depth, and we do not know how reduced buoyancy at greater depths affects force requirements. Lower buoyancy would allow the birds to direct more force forwards during the upstroke instead of downwards. A steeper dive angle would make it possible for the birds to use the downstroke to produce a downward-directed force to counteract buoyancy and, thereby, allow the upstroke to be used for thrust production. Further studies of free-swimming alcids are clearly needed.

This study was made possible thanks to Páll Marvin Jónsson at the University of Iceland's Fisheries Research Unit at the Vestman Islands, who provided lodging and transportation and caught the birds. We thank Jon-Ingi Ragnarson and family for help with logistics and for lodging in Reykjavik. We also thank Åke Norberg for valuable scientific discussions and advice, Ulla Lindhe Norberg for comments on the manuscript and Sven Nilsson for helping with the three-dimensional image. This study was funded by Kungliga Vetenskaps- och Vitterhetssamhället i Göteborg, H. Ax:son Johnson stiftelse, Kungliga och Hvitfeldska stipendiestiftelsen, Kungliga vetenskapsakademien (Hierta-Retzius), Långmanska Kulturfonden, and W. och M. Lundgren vetenskapsfond (all to L.C.J.).

References

- Bannasch, R. (1995). Hydrodynamics of penguins – an experimental approach. In *The Penguins* (ed. P. Dann, I. Norman and P. Reilly), pp. 141–176. Surrey, UK: Beatty & Sons.
- Burkett, C. W. (1989). Reductions in induced drag by the use of aft swept wing tips. *Aeronaut. J.* **93**, 400–405.
- Clark, B. D. and Bemis, W. (1979). Kinematics of swimming of penguins at the Detroit Zoo. *J. Zool., Lond.* **188**, 411–428.

- Croll, D. A. and McLaren, E.** (1993). Diving metabolism and thermoregulation in Common and Thick-billed murre. *J. Comp. Physiol. B* **163**, 160–166.
- Dabelow, A.** (1925). Die Schwimmanpassung der Vögel. Ein Beitrag zur biologischen Anatomie der Fortbewegung. *Jb. Morph. Mikroskop. Anat.* **54**, 288–321.
- Ellington, C. P.** (1984). The aerodynamics of hovering insect flight. IV. Aerodynamic mechanisms. *Phil. Trans. R. Soc. Lond. B* **305**, 79–113.
- Goodge, W. R.** (1959). Locomotion and other behavior of the Dipper. *Condor* **61**, 4–17.
- Hawkins, P. A. J., Butler, P. J., Woakes, A. J. and Speakman, J. R.** (2000). Estimation of the rate of oxygen consumption of the common eider duck (*Somateria mollissima*), with some measurements of heart rate during voluntary dives. *J. Exp. Biol.* **203**, 2819–2832.
- Hui, C. A.** (1988). Penguin swimming. I. Hydrodynamics. *Physiol. Zool.* **61**, 333–343.
- Humphrey, P. S.** (1958). Diving of a captive common eider. *Condor* **60**, 408–410.
- Kovacs, C. E. and Meyers, R. A.** (2000). Anatomy and histochemistry of flight muscles in a wing-propelled diving bird, the Atlantic Puffin, *Fratercula arctica*. *J. Morphol.* **244**, 109–125.
- Lanczos, C.** (1956). *Applied Analysis*. Englewood Cliffs, NJ: Prentice Hall. 539pp.
- Liu, P. F. and Bose, N.** (1999). Hydrodynamic characteristics of a lunate shape oscillating propulsor. *Ocean Engineering* **62**, 519–529.
- Lovvorn, J. R., Croll, D. A. and Liggins, G. A.** (1999). Mechanical versus physiological determinants of swimming speeds in diving Brünnich's guillemots. *J. Exp. Biol.* **202**, 1741–1752.
- Lovvorn, J. R. and Jones, D. R.** (1991). Body mass, volume and buoyancy of some aquatic birds and their relation to locomotor strategies. *Can. J. Zool.* **69**, 2888–2892.
- Lovvorn, J. R. and Jones, D. R.** (1994). Biomechanical conflicts between adaptations for diving and aerial flight in estuarine birds. *Estuaries* **17**, 62–75.
- Norberg, U. M.** (1996). Energetics of flight. In *Avian Energetics and Nutritional Ecology* (ed. C. Carey), pp. 199–249. New York: Chapman & Hall.
- Rayner, J. M.** (1988). Form and function in avian flight. *Curr. Ornithol.* **5**, 1–66.
- Rayner, J. M.** (1995). Dynamics of the vortex wakes of flying and swimming vertebrates. *Symp. Soc. Exp. Biol.* **49**, 131–155.
- Ryan, P. G. and Nel, D. C.** (1999). Foraging behaviour of diving petrels Pelecanoides. *Emu* **99**, 72–74.
- Spring, L.** (1971). A comparison of functional and morphological adaptations in the Common murre (*Uria aalge*) and Thick-billed murre (*Uria lomvia*). *Condor* **73**, 1–27.
- Stettenheim, P.** (1959). Adaptations for underwater swimming in the Common murre (*Uria aalge*). PhD thesis, Ann Arbor, University of Michigan. 295pp.
- Storer, R. W.** (1960a). Evolution in the diving birds. *Int. Ornithol. Congr.* **12**, 694–707.
- Storer, R. W.** (1960b). Adaptive radiation in birds. In *Biology and Comparative Physiology of Birds*, vol. 1 (ed. A. J. Marshall), pp. 15–55. New York: Academic Press.
- van Dam, C. P.** (1986). Drag-reduction of aft-swept wing tips. *AIAA Paper* **86-1824**, 327–338.
- van Dam, C. P.** (1987). Efficiency characteristics of crescent-shaped wings and caudal fins. *Nature* **325**, 435–437.
- van Dam, C. P., Vijgen, P. M. H. W. and Holmes, B. J.** (1991a). Aerodynamic characteristics of crescent and elliptic wings at high angles of attack. *J. Aircraft* **28**, 253–260.
- van Dam, C. P., Vijgen, P. M. H. W. and Holmes, B. J.** (1991b). Experimental investigation on the effect of crescent planform on lift and drag. *J. Aircraft* **28**, 713–720.
- Vogel, S.** (1994). *Life in Moving Fluids*. Princeton, NJ: Princeton University Press. 467pp.
- Watanuki, Y. and Burger, A. E.** (1999). Body mass and dive duration in alcids and penguins. *Can. J. Zool.* **77**, 1838–1842.